Journal of the Korean Nuclear Society
Volume 36, Number 3, pp.203~209, June, 2004

Measurements of In-phantom Neutron Flux Distribution at the HANARO BNCT Facility

Myong Seop Kim, Sang Jun Park, and Byung Jin Jun
Korea Atomic Energy Research Institute
150, Deokjin-dong, Yuseong-gu, Daejeon, 305-353, Korea
mskim@kaeri.re.kr

(Received May 29, 2003)

Abstract

In-phantom neutron flux distribution is measured at the HANARO BNCT irradiation facility. The measurements are performed with Au foil and wires. The thermal neutron flux and Cd ratio obtained at the HANARO BNCT facility are 1.19×10^9 n/cm^{2}s and 152, respectively, at 24 MW reactor power. The measured in-phantom neutron flux has a maximum value at a depth of 3 mm in the phantom and then decreases rapidly. The maximum flux is about 25 % larger than that of the phantom surface, and the measured value at a depth of 22 mm in the phantom is about a half of the maximum value. In addition, the neutron beam is limited well within the aperture of the neutron collimator. The two-dimensional in-phantom neutron flux distribution is determined. Significant neutron irradiation is observed within 20 mm from the phantom surface. The measured neutron flux distribution can be utilized in irradiation planning for a patient.

Key Words : BNCT, in-phantom neutron flux distribution, HANARO, irradiation facility, Au foil

1. Introduction

Boron neutron capture therapy(BNCT) is a promising method of cancer treatment in principle, which kills cancer cells selectively by the use of a cancer seeking boron compound and neutron irradiation[1,2]. The ranges of resultant particles from the boron-neutron reaction are very similar to the cell size[3]. Therefore, the killing of a boron-lined tumor cell is possible without affecting the healthy cells. This therapy is expected to be very effective for the malignant brain tumor - glioblastoma multiforme, for which no successful human treatment has been developed, and worldwide research using the research reactor and accelerator is on going[4,5,6].

Because the biological effect of a neutron is almost constant up to 10 keV, but rises rapidly above that level, the use of epithermal neutrons just below 10 keV is supposed to be the most effective. Since the irradiation of epithermal neutrons causes a thermal neutron peak at depth of about 2.5 cm, such irradiation can be used without debulking. Therefore, in the USA and Europe, whole brain irradiation using epithermal neutrons has been studied; while in Japan, local

irradiation after debulking has been successful in several cases.

In HANARO, a 30 MW research reactor, due to its design characteristics, sufficient epithermal neutrons for BNCT cannot be obtained, but sufficient thermal neutrons can be obtained by means of a filtering method[7].

For the last several years, the design and installation of the HANARO BNCT irradiation facility have been completed, and the structure of the irradiation room has been installed[8,9]. The thermal neutron facility can be used for local irradiation and for research before clinical trials, such as small animal irradiation.

The capture cross-section for the $B^{10}(n,\alpha)Li^7$ reaction decreases to $E^{-1/2}$, where E is the neutron energy, and so the neutron which kills the tumor cell is a thermal neutron. Therefore, the distribution of thermal neutron flux in the brain is a major factor in determining the efficiency of BNCT.

In this study, neutron fluxes are measured at various conditions in the facility, and the two-dimensional in-phantom thermal neutron distribution is experimentally determined.

2. Apparatus and Experimental Procedures

At HANARO, a neutron irradiation facility for BNCT was installed using a typical tangential beam port whose nose is located in the thermal neutron peak area of the heavy water reflector. It consists of a water shutter, a fast neutron and gamma ray filter, a liquid nitrogen cooling system, a beam collimator, and shieldings. Figure 1 shows the layout of the HANARO BNCT irradiation facility.

A water shutter of 135 cm in length enables experimenters to use the facility without having to shutdown the reactor; therefore, different research activities within HANARO can be performed simultaneously. A radiation filtering system, using silicon and bismuth single crystals, is adopted in order to obtain a high thermal neutron flux and low fast neutron and gamma ray fluxes. The thermal neutron passes better than the fast neutron through the Si single crystal, and the bismuth used as the gamma ray filter has similar characteristics when it has a crystal structure. In addition, the penetration of thermal neutrons is greatly enhanced when the single crystals are cooled down to the temperature of liquid nitrogen (LN_2). Therefore, the radiation filter consists of a Si single crystal, 40 cm in length and 20 cm in diameter, a Bi single crystal, 15 cm in length and 10 cm in diameter, and a LN_2 cooling system. The thermal neutron beam extracted from the filter should be collimated for focused irradiation. The cone shape collimators are manufactured by sintering the mixture of 95 % Li-6 enriched Li_2CO_3 and polyethylene powder[10]. The diameter of the collimator used in the present experiments is 146.7 mm. The shielding materials used in the facility are polyethylene, lead, Bi poly-crystal, etc. In order to monitor the neutron and gamma rays, the fission chamber and the gamma ion chamber are positioned inside the shielding.

Experimental measurements of the neutron flux are performed using bare and cadmium covered gold foils and wires. The thickness of the Au foil used is 0.001 inches, and its diameter is 0.5 inches; the diameters of the Au wires are either 0.1 or 0.254 mm. The neutron flux is measured at a reactor power of 24 MW.

The time necessary to open the water shutter for neutron irradiation is about 3 min, and the time required to close it is about 2 min. Therefore, the irradiation time cannot be determined clearly, unlike when using a quick shutter system. Therefore, in order to investigate the variation of the neutron irradiation rate at the position of the Au flux monitor during the operation of a water shutter, the variation of the count rate of the

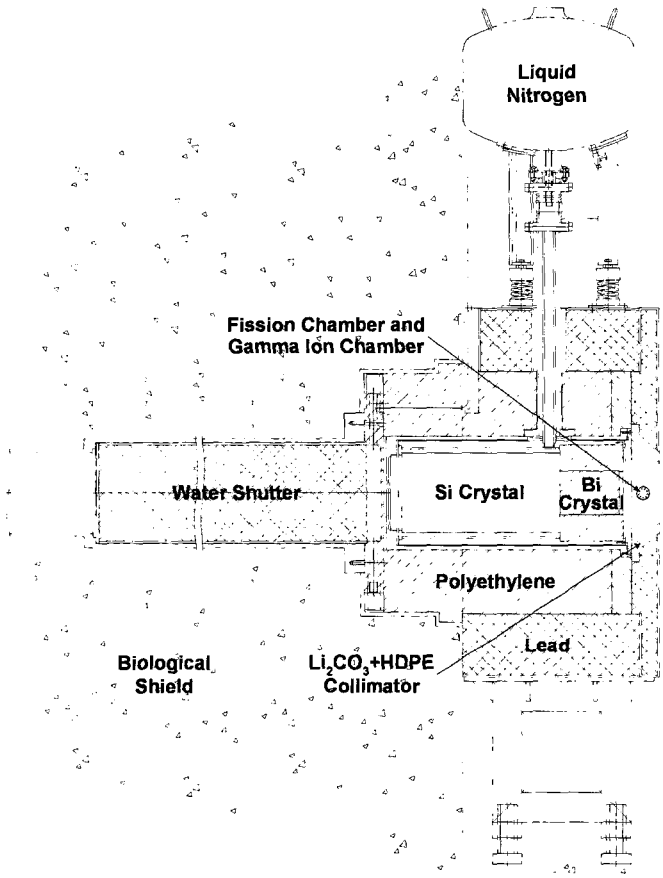

Fig. 1. Layout of the BNCT Irradiation Facility of HANARO

fission chamber is measured during the shutter operation.

The activity of the irradiated Au sample is measured using a calibrated high purity germanium detection system. The uncertainty in determining the activity is within 2 %, and the dominant factor is the uncertainty of the standard source activity.

The phantom used in the experiments is a 300 × 300 mm^2 rectangular solid slab phantom, and its specifications are represented in Table 1.

In the first stage of the experiments, the free beam neutron flux and Cd ratio are measured at the exit of the beam collimator with the variation of the LN_2 cooling condition of the radiation filter. In

Table 1. The Specifications of the Solid Slab Phantom

Parameters	Figures
Name	Solid slab phantom Type-29672
Manufacturer	PTW-Freiburg
Radiation qualities	Photons ^{60}Co ··· 20 MV Electron 4 MeV ··· 25 MeV
Outer dimensions	300 mm × 300 mm
Material	Polystyrene(C_8H_8) containing 2% by mass TiO_2
Density	1.045 g/cm^3
Slab thickness	1 mm, 2 mm, 5 mm, 10 mm
Tolerance of slab thickness	±0.1 mm
Electron density	0.012 times higher than electron density of water
Mean Z/A value	0.536

the second stage, the two-dimensional in-phantom neutron flux distribution is measured. For the mapping of the neutron flux distribution inside the phantom, a number of Au monitors are located at the proper positions inside the slab phantom.

3. Results

Figure 2 shows the changes in fission chamber count rates during the opening and closing of the water shutter. It was found that the response of the fission chamber count rate to the water shutter operation is linear. Therefore, we suppose that the neutron irradiation at the Au sample position varies as shown in figure 3. The neutron flux can be deduced from the activity of the Au monitor as follows.

$$\phi_0 = \frac{\lambda}{N_m \sigma} \frac{A(t_4)}{\left[\frac{1}{t_2}(e^{-\lambda t_4} - e^{\lambda(t_2 - t_4)}) + \frac{1}{t_3 - t_4}(e^{\lambda(t_2 - t_4)} - 1)\right]} \quad (1)$$

where, N_m is the number of Au nucleus at the sample, σ is the radiative capture cross-section,

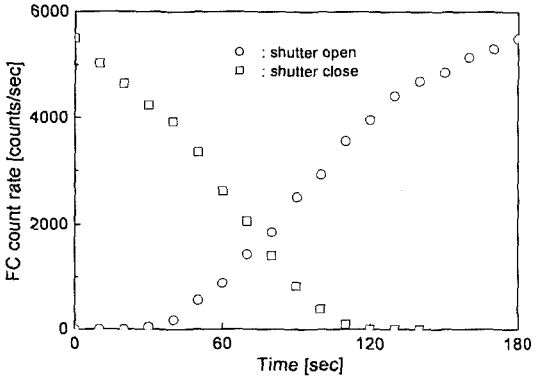

Fig. 2. Changes in Fission Chamber Count Rates During the Opening and the Closing of the Water Shutter

and λ is the decay constant of Au-198.

For the case of a one-directional neutron beam, the neutron attenuation effect inside the Au flux monitors is calculated. The correction factors are

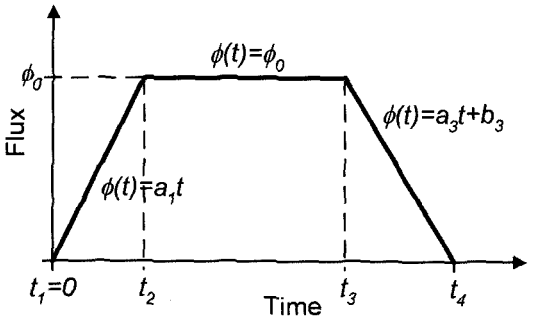

Fig. 3. The Variation of the Neutron Irradiation at the Au Sample Position

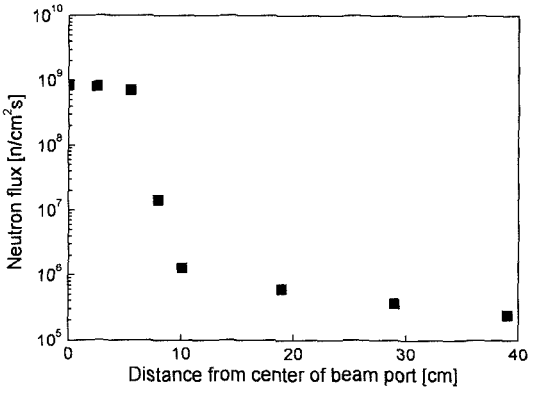

Fig 4. The Measured Thermal Neutron Flux at the Exit Position of the Beam Collimator

0.9758 for the Au wire with a 0.1 mm diameter and 0.9402 for the Au wire with a 0.254 mm diameter. In the case of an Au foil with a thickness of 0.0254 mm, the correction is negligible. The deduced neutron flux is corrected by multiplying this correction factor.

Figure 4 shows the neutron flux measured using Au foils at the exit position of the beam collimator. The neutron irradiation can be limited well within the diameter of the beam collimator.

Figure 5 shows the relative neutron fluxes measured using bare Au wire and Cd covered Au wire. As the figure shows, it was confirmed that both the thermal and fast neutron irradiations outside the collimation area, using Li_2CO_3 and polyethylene, are negligible.

Table 2. The Thermal Neutron Flux and Cd Ratio Measured at Several Experimental Conditions

Sequential number	Experimental condition				Thermal neutron flux [n/cm^{2}s]	Cd ratio
	Cooling		Phantom			
	with	without	with	without		
1		o		o	8.34×10^8	104
2		o		o	8.77×10^8	
		o	o		1.82×10^9	
3	o			o	1.04×10^9	
	o		o		2.23×10^9	
4	o			o	1.12×10^9	
5	o			o	1.19×10^9	
6	o			o	1.15×10^9	
7		o		o	8.13×10^8	
8		o	o		1.74×10^9	
9	o			o	9.69×10^8	152
	o		o		2.08×10^9	
10	o			o	1.06×10^9	145

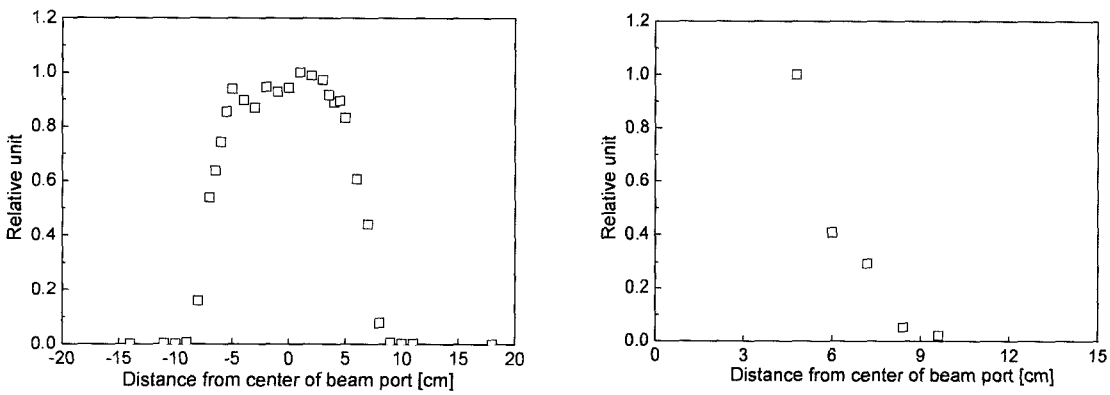

Fig. 5. The Relative Neutron Fluxes Measured Using Bare Au Wire(a) and Cd Covered Au Wire(b)

The absolute neutron flux and Cd ratio measured at several experimental conditions are represented at Table 2. The uncertainty of the measured flux is within 2.5 %. In spite of the same experimental conditions, the measurements are in the broad range of about 20 %. This discrepancy is attributed to the cooling status of the radiation filter and the conditions within the reactor core, such as the disposition of the nuclear fuel. When the radiation filter is cooled with liquid nitrogen, the neutron flux and Cd ratio increase to 30 % and 50 %, respectively, in contrast to the measurements before cooling. The measured neutron flux at the surface of the phantom increases by twofold or more than the measured neutron flux without the phantom.

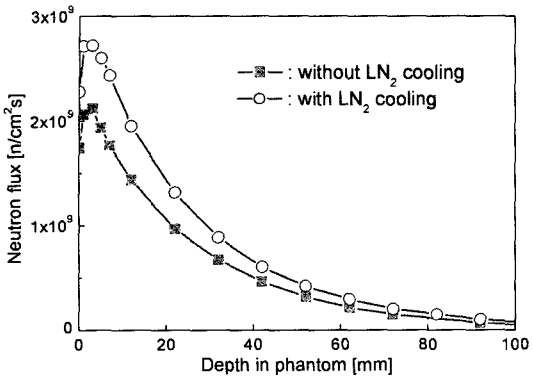

Fig. 6. The Measured Neutron Flux Distribution as a Function of Depth in the Phantom Through the Central Axis of Beam Exit

From the above results, it was confirmed that the thermal neutron flux and the Cd ratio that can be obtained at the HANARO BNCT facility are 1.19 $\times 10^9$ n/cm^{2}s and 152, respectively, at 24 MW reactor power.

Figure 6 shows the measured neutron flux distribution as a function of depth in the phantom, through the central axis of the beam exit. As shown in figure 6, the thermal neutron flux reaches a maximum near a 3 mm depth in the phantom, and then decreases rapidly. The maximum flux is about 25 % larger than that of the phantom surface, and the measured value at a depth of 22 mm in the phantom is about a half of the maximum value. For the measurements with and without LN_2 cooling, the neutron flux distributions tend to change similarly. When the radiation filter is cooled by LN_2, the thermal neutron flux is 30% larger than that without cooling over the whole depth.

The measured two-dimensional in-phantom neutron flux distribution is shown in figure 7. Significant neutron irradiation is observed within 20 mm from the phantom surface. The area enclosed by the isoflux line of 2×10^9 n/cm^{2}s or more is located within a 12 mm depth in the phantom. The 2×10^9 n/cm^{2}s flux is about 77 % relative to the maximum flux. The neutron flux

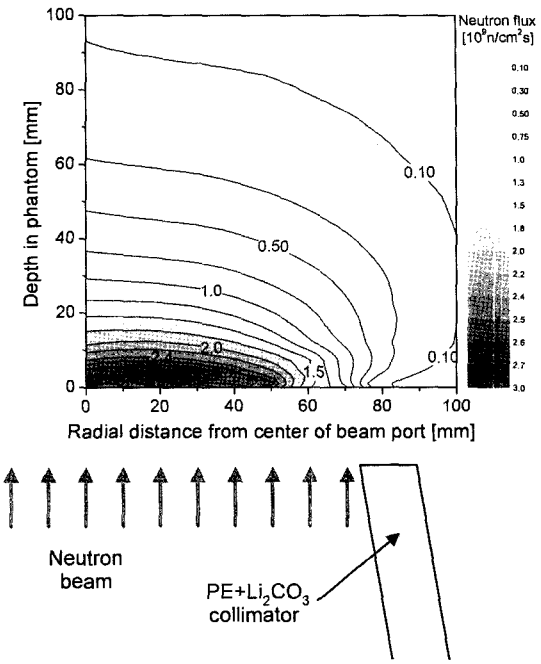

Fig. 7. The Measured Two-dimensional In-phantom Thermal Neutron Flux Distribution

distribution near the phantom surface looks as though it has a double isoflux area enclosed by the 2.6×10^9 line in the lateral direction; this is caused by the neutron scattering from the collimator. This area has the maximum neutron flux. The isoflux area enclosed by the 2.6×10^9 line has a maximum width of 33 mm in the lateral direction, and it is 44 % of the collimator exit diameter. The thermal neutron flux falls off rapidly with an increase in the depth in the phantom.

The measured neutron flux distribution is utilized in irradiation planning, such as determining the optimal size of the collimator and the optimal position for the patient' s head [11,12,13].

4. Conclusions

Neutron fluxes were measured at various conditions in the HANARO BNCT facility, and the two-dimensional in-phantom thermal neutron distributions were experimentally determined. The

measured thermal neutron flux and Cd ratio were 1.19×10^9 n/cm^{2}s and 152, respectively, at 24 MW reactor power. The measured in-phantom neutron flux had a maximum value at a depth of 3 mm in the phantom and then decreased rapidly. The observed neutron flux distribution can be useful in planning irradiation for a patient.

Acknowledgment

This study has been carried out with the support of the Ministry of Science and Technology (MOST), Republic of Korea.

Reference

1. D.N. Slatkin, "A History of Boron Neutron Capture Therapy of Brain Tumors", Brain, 114, 1609 (1991).
2. "Boron-Neutron Capture Therapy for Tumors", edited by H. Hatanaka, Nishimura Co. Ltd., (1986).
3. H. Yanagië, T. Tomita, H. Kobayashi, Y. Fujii, Y. Nonaka, Y. Saegusa, K. Hasumi, M. Eriguchi, T. Kobayashi and K. Ono, "Inhibition of human pancreatic cancer growth in nude mice by boron neutron capture therapy", British Journal of Cancer 75(5), 660 (1997).
4. "Advances in Neutron Capture Therapy Volume I, Medicine and Physics", Proceedings of the Seventh International Symposium on Neutron Capture Therapy for Cancer, ed. B. Larsson, J. Crawford and R. Weinreich, Zurich, Switzerland (1996).
5. "Research and Development in Neutron Capture Therapy", Proceedings of the 10th International congress on Neutron Capture Therapy, ed. W. Sauerwein, R. Moss and A. Wittig, Essen, Germany (2002).
6. C.Y. HAN, J.K. KIM, and K.S. CHUNG, "An Epithermal Neutron Beam Design for BNCT Using ^{2}H(d,n)^{3}He Reaction", Journal of the Korean Nuclear Society 31(5), 512 (1999).
7. B.C. Lee, S.J. Park, M.S. Kim and B.J. Jun, "BNCT Facility Development in HANARO", Proceedings of the International Group on Research Reactors 9th meeting(IGORR9), Sydney, Australia (2003).
8. S.Y. Hwang, M.S. Kim, B.J. Jun, J.B. Lee, S.J. Park, B.H. Lee, B.C. Lee, J.H. Lee, K.H. Lim and M.J. Kim, "Installation of BNCT Irradiation Facility and Measurement of Neutron and Gamma-ray Leakages", Proceedings of the Korean Nuclear Society Spring Meeting, Korea (2001) (in Korean).
9. M.S. Kim, S.J. Park, B.C. Lee and B.J. Jun, "Neutron Flux Measurements of Irradiation Facility with BNCT Neutron Filter of Room Temperature", Proceedings of the Korean Nuclear Society Spring Meeting, Korea (2002) (in Korean).
10. G.Y. Lee, S.Y. Hwang and B.J. Jun, "Development of Mixed Shielding Materials using Li-6 enriched Lithium Carbonate and HDPE for the BNCT Beam Collimator of the HANARO", Proceedings of the Korean Association for Radiation Protection Autumn Meeting, Korea (2001) (in Korean).
11. T. Yamamoto, A. Matsumura, K. Yamamoto, H. Kumada, Y. Shibata and T. Nose, "In-phantom two-dimensional thermal neutron distribution for intraoperative boron neutron capture therapy of brain tumours", Phys. Med. Biol. 47, 2387 (2002).
12. K. Tanaka, T. Kobayashi, Y. Sakurai, Y. Nakagawa, S. Endo and M. Hoshi, "Dose distributions in a human head phantom for neutron capture therapy using moderated neutrons from the 2.5 MeV proton-^{7}Li reaction or from fission of ^{235}U", Phys. Med. Biol. 46, 2681 (2001).
13. Y. Sakurai and T. Kobayashi, "Characteristics of the KUR Heavy Water Neutron Irradiation Facility as a neutron irradiation field with variable energy spectra", Nucl. Instr. and Meth. A453, 569 (2002).